

NY

# Technical Memorandum No. 33-186

## Possible Meteoroid Hazard to Solid-Propellant Rocket Motors

Carol L. Robillard

FACILITY FORM 802	N 67 - 21166	
	(ACCESSION NUMBER)	(THRU)
	28	1
	(PAGES)	(CODE)
	CR-83118	28
	(NASA CR OR TMX OR AD NUMBER)	(CATEGORY)



JET PROPULSION LABORATORY  
CALIFORNIA INSTITUTE OF TECHNOLOGY  
PASADENA, CALIFORNIA

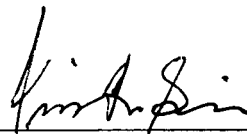
November 1, 1964

807-42301

*Technical Memorandum No. 33-186*

*Possible Meteoroid Hazard to Solid-  
Propellant Rocket Motors*

*Carol L. Robillard*



---

Winston Gin, Chief  
Solid Propellant Engineering Section

**JET PROPULSION LABORATORY  
CALIFORNIA INSTITUTE OF TECHNOLOGY  
PASADENA, CALIFORNIA**

November 1, 1964

**Copyright © 1964  
Jet Propulsion Laboratory  
California Institute of Technology**

**Prepared Under Contract No. NAS 7-100  
National Aeronautics & Space Administration**

## CONTENTS

I. The Meteoroid Environment .....	2
II. Hypervelocity Penetration Data .....	6
III. Combination of the Penetration and Flux Equations for Meteoroid Masses Greater Than $10^{-6}$ g .....	10
IV. Applicability of the <i>Explorer XVI</i> Data .....	13
V. Conclusions .....	19
Nomenclature .....	23
References .....	24

## TABLES

1. Penetrating-flux equations .....	10
2. Probability of sustaining one or more critical penetrations during an unmanned Mars mission .....	20
3. Pressure vessels; effect of size and chamber pressure on probability of penetration .....	22

## FIGURES

1. Whipple's comparison of flux equations .....	3
2. Hypervelocity penetration data .....	6
3. <i>Explorer XVI</i> : spacecraft configuration .....	13
4. <i>Explorer XVI</i> : normalized accumulated punctures vs time in orbit .....	15
5. <i>Explorer XVI</i> : near-Earth flux of penetrating particles vs target thickness.....	16
6. Near-Earth flux of penetrating particles vs penetration depth: comparison of calculated values with <i>Explorer XVI</i> values .....	17

## ABSTRACT

Available data on hypervelocity penetration and on near-Earth and deep-space meteoroid environment were examined, and an attempt to determine the probable extent of meteoroid hazard to solid-propellant rocket motors was made.

The probabilities of critical penetration for a small and a large solid-propellant spacecraft motor were estimated for a typical unmanned Mars mission. Although these values may be in error by more than an order of magnitude, they do show a basis for concern, and they suggest that higher chamber pressures at a small loss in performance may be a good investment.

It was found that the most interesting observations about probability of puncture of solid-propellant rocket motor cases depend only on the slope of the penetrating-flux curve and not on the magnitude of the meteoroid flux. The probability of puncture is proportional to the slope ( $-n$ ) of the penetrating meteoroid flux vs penetration-depth curve. Provided  $n$  is greater than two, the probability of puncture decreases with increasing motor-case radius, and with increasing chamber pressure.

## I. THE METEOROID ENVIRONMENT

Calculation of meteoroid damage requires a knowledge of the meteoroid environment, which includes meteoroid concentration, mass, density, position, and velocity, in combination with a valid penetration theory and failure criteria.

There is general agreement that the meteoroid concentration (number of particles per unit volume) varies with position in space. A vague outline of a geometrical model emerges from available light-scattering data, to wit:

1. Almost all matter is concentrated in the plane of the ecliptic ( $\pm 20^\circ$ ).
2. The deep-space meteoroid concentration in the plane of the ecliptic varies inversely with increasing distance from the Sun, except between Mars and Jupiter.
3. The near-Earth meteoroid concentration is greater than that otherwise present at 1 AU in the plane of the ecliptic and away from Earth's gravity field.
4. The near-Earth particle concentration varies inversely with increasing distance from the Earth.

Most of the near-Earth meteoroid data have been reported in terms of cumulative meteoroid flux as a function of mass; that is

$$N = Cm^{-Z}$$

where  $N$  is the flux of all particles of mass  $m$ , or greater, and flux is defined as the number of particles/unit area/unit time. It is uniformly assumed that the flux is omnidirectional.

Many techniques have been employed to determine near-Earth flux as a function of mass. Almost all of these techniques have one major shortcoming: they require assumptions concerning the other meteoroid characteristics, such as density, shape, and velocity, to calculate the mass. Earth satellite and rocket-probe experiments employing grids, microphones, or impact plates have been designed to study very small particles ( $\leq 10^{-7}$  g). Available data for larger meteoroids ( $\geq 10^{-5}$  g) have been acquired by using visual, photographic and radio techniques from Earth.

Whipple (Ref. 1) compiled cumulative flux vs mass curves from these many sources (Fig. 1). There are two important points associated with these data:

1. The data suggest that there is a significant change in the slope for near-Earth flux in the region of meteoroid mass of  $10^{-8}$  to  $10^{-12}$  g.
2. Our best estimate of the smallest meteoroid mass which would penetrate one-half the thickness of a 0.001-in.-thick steel target is approximately  $10^{-6}$  g. Therefore, for solid rocket motors, we are most interested in the data for meteoroid masses of about  $10^{-6}$  g, or greater; that is, for near-Earth flux, the data acquired by using visual, photographic and radio techniques from Earth.

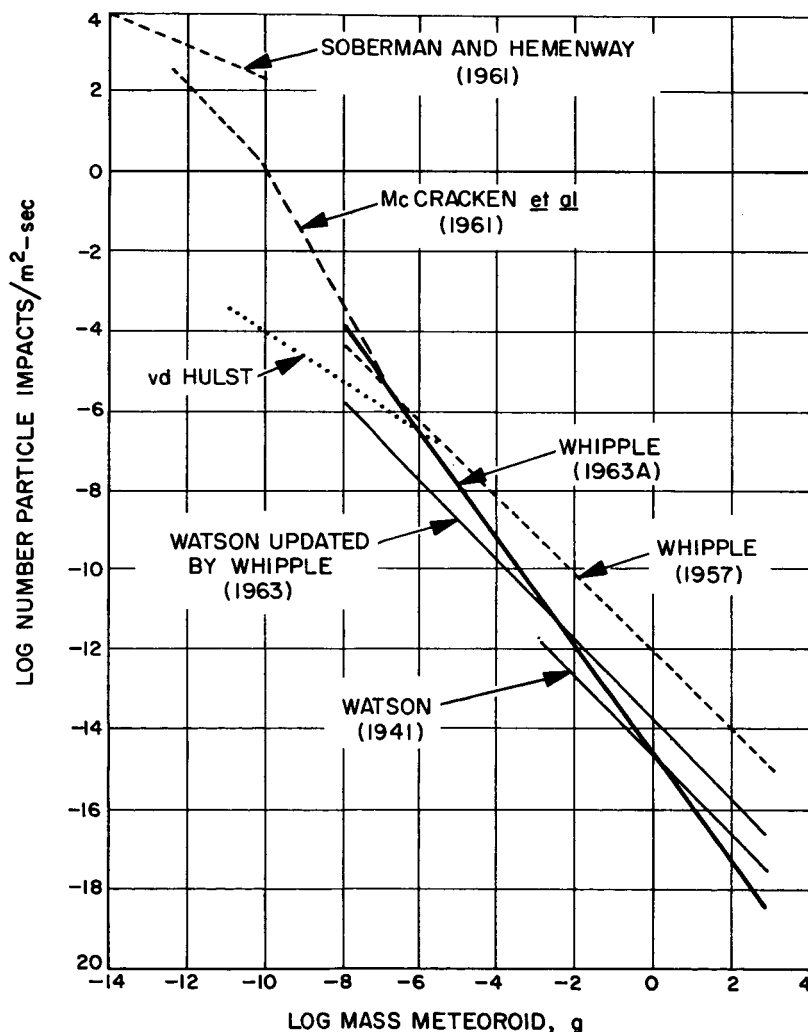


Fig. 1. Whipple's comparison of flux equations

The Whipple 1963A curve (Fig. 1) represents the most recent near-Earth data for meteoroids near the mass range of interest. Whipple derived values for the mean velocity and density of these meteoroids of 22 km/sec and 0.44 g/cm<sup>3</sup>, respectively. The Whipple flux equation contains a correction term for meteoroid-density estimates other than 0.44 g/cm<sup>3</sup>. The net effect of this correction term is that doubling the density decreases the flux for any given meteoroid mass by almost an order of magnitude. The Whipple equation is

$$N = m^{-1.34} \times \left( \frac{0.443}{\rho} \right)^{2.68} \times 10^{-14.48}$$

where

$$\rho = \text{new value of meteoroid density, g/cm}^3$$

$$m = \text{mass, g}$$

$$N = \text{cumulative flux, number of particles/m}^2\text{-sec}$$

The Whipple 1963A curve (Fig. 1) represents his best estimate of meteoroid density, 0.44 g/cm<sup>3</sup>.

Unfortunately, the deep-space environment is even less well defined than the near-Earth environment; however, the near-Earth flux may decrease with increasing distance from the Earth. Any decrease in flux from the near-Earth to the deep-space value is expected to be continuous and to extend through approximately 100 Earth radii. The expected decrease is, however, mass dependent; that is, the ratio

$$\frac{\text{near-Earth flux}}{\text{deep-space flux}}$$

should decrease as the mass increases. For masses of 10<sup>-1</sup> g, and above, it is generally agreed that the ratio of near-Earth to deep-space flux is of the order of one. Jaffe (Ref. 2) selected a deep-space flux vs mass relation, which was based on Beard's solar-corona data, in conjunction with the near-Earth data for larger particles available at that time; e.g., Whipple's 1957 flux curve. The selected flux equation for deep space was

$$N = m^{-0.69} \times 10^{-12.4}$$

Based on Whipple's 1957 near-Earth flux, the above equation yields values for the ratio



near-Earth flux  
deep-space flux

of approximately  $10^2$  at  $m = 10^{-6}$  g, and 1 at  $m = 10^{-1}$  g.

## II. HYPERVELOCITY PENETRATION DATA AND FAILURE CRITERIA

A particle impacting a target primarily results in crater formation, which is usually described in terms of penetration depth. The secondary effect is spallation. Both penetration (or crater formation) and spallation should be taken into account in formulating the failure criteria.

Meteoroids can encounter Earth's upper atmosphere with velocities of approximately 11 to 73 km/sec. On the other hand, the vast majority of hypervelocity penetration data is for velocities under 5 km/sec. Data near the velocity value adopted by Whipple, 22 km/sec, are relatively rare. Scully's data<sup>1,2</sup> are shown in Fig. 2. These data indicate that the relative resistance of any given set of materials to penetration is dependent upon the velocity. An extreme example of the velocity effect can be seen with beryllium, which is

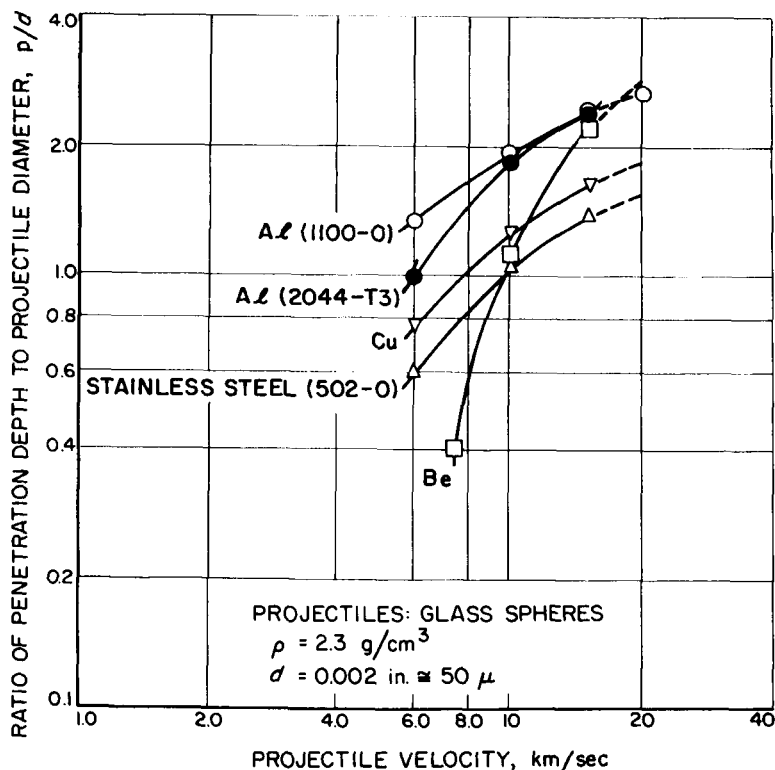


Fig. 2. Hypervelocity penetration data

<sup>1</sup>Unpublished data, courtesy of Mr. Norman Scully, Space Science Laboratories, North American Aviation, Inc.

<sup>2</sup>For Al (1100-O), the penetration data extend to 20 km/sec. For the other metals, the data extend to 15 km/sec, and the curves have been extrapolated to 20 km/sec.

the most resistant to penetration at 8 km/sec and the least resistant at 20 km/sec. Unfortunately, Scully obtained no data to show the effect of variations in density, diameter, or shape of the projectile. Note also that these data are for penetration into semi-infinite solids, rather than into thin sheets,<sup>3</sup> and for an incidence angle of 90 deg.

Note that Scully's penetration data were presented in the form

$$\left( \frac{P}{d} \right)_{\rho, d} = f(v)$$

However, for some given value of velocity, these penetration data can be converted to the form

$$m = f(P)$$

by combining the following two equations

$$\left( \frac{P}{d} \right)_{v, \rho, d} = C$$

and

$$\rho = \frac{m}{0.5236 d^3}$$

or

$$d = \left( \frac{m}{0.5236 \rho} \right)^{1/3}$$

---

<sup>3</sup>A semi-infinite solid is one for which no change in penetration depth is observed when its thickness is increased.

where

$C$  is a constant for some given target material, and projectile velocity, density, and diameter;

$\rho$  is the density of the projectile;

$0.5236 d^3$  is the volume of a *spherical* projectile.

The resulting penetration equations for a projectile velocity of 20 km/sec, with a density of 2.3 g/cm<sup>3</sup> and a diameter of 0.002 in. are

$$m = \left( \frac{P}{1.69} \right)^3 \text{ for a semi-infinite copper target at normal incidence}$$

$$m = \left( \frac{P}{1.41} \right)^3 \text{ for a semi-infinite stainless steel target at normal incidence}$$

Penetration data for velocities lower than 15 km/sec indicate that projectiles penetrate 1.2 to 1.9 times further into a thin sheet than into a semi-infinite solid. The very small amount of data existing for penetration as a function of incidence angle suggests that penetration depth is proportional to the sine of the incidence angle. If it is assumed that

$$P_{\text{thin}}/P_{\text{thick}} = 1.5$$

and that

$$\bar{\theta} \text{ incidence} = 45 \text{ deg } (\sin 45 \text{ deg} \cong 0.7)$$

then these two effects cancel each other out. That is, the penetration depth for a projectile impinging on a thin target at a 45-deg incidence angle is approximately equal to the penetration depth for a projectile impinging on a thick target at 90-deg incidence angle. This approximation is admittedly crude, but it may have to be used in the absence of data.

The effect of projectile density on penetration depth at velocities greater than 5 km/sec must also be approximated. Herrmann and Jones suggest that the ratio  $P/d$  is proportional to the two-thirds power of projectile density; however, their correlation is based almost entirely on data for velocities less than

5 km/sec. If it is presumed that this correlation holds at high velocities, then, for a projectile of density of approximately  $0.44 \text{ g/cm}^3$  (Whipple's estimate), the penetration equation for stainless steel becomes

$$m = \left( \frac{P}{0.837} \right)^3$$

And, finally, a small amount of recent data reported by Manned Spacecraft Center (for spherical projectiles at constant density and 7 km/sec) indicates that the ratio  $P/d$  increases with increasing projectile diameter.<sup>4</sup> The effect of projectile shape is unknown.

With respect to failure criteria, the practical question to determine is: What kind and degree of meteoroid damage constitutes failure in solid propellant cases? Would one penetration cause failure, or would it take three? On the other hand, it may be asked whether or not a partial perforation (i.e., one penetration to one-half or one-third the wall thickness with attendant spallation) constitutes failure.

There are no equations comparable to those describing penetration for describing spallation or cracking caused by meteoroid impact. Dubin (Ref. 3) states that spallation can occur even though the projectile penetrates only to a small fraction of the sheet thickness, and that the diameter of the section spalled is usually several times the sheet thickness, with the spall thickness usually one-tenth to one-half the thickness of the sheet. Brittle materials can sustain much greater damage than ductile materials when a projectile penetrates only to a small fraction of the sheet thickness.

Little data are presently available to determine failure criteria. For solid-propellant motors, the answer lies in determining the effects of meteoroid penetration and spalling on the mechanical integrity of the motor case on ignition, and of case-to-liner bonds. In practice, the critical fraction of case thickness (for example, one-half) will probably vary with case material, with wall thickness, and with design criteria (safety factor and pad). It is expected to be a strong function of the material brittleness and notch sensitivity.

---

<sup>4</sup>The equation given was  $\left( \frac{P}{d} \right)_{v,\rho} = 2.072 d^{0.0563}$  (with  $d$  in microns). The projectile and target materials and densities were unspecified.

### III. COMBINATION OF THE PENETRATION AND FLUX EQUATIONS FOR METEOROID MASSES GREATER THAN $10^{-6}$ g

As shown in Table 1, combining the penetration equations [ $m = f(P)$ ] with the cumulative flux equations [ $N = f(m)$ ] yields the flux of meteoroids, which penetrate to a depth  $P$ , or greater, [ $N$  (penetrating) =  $\phi = f(P)$ ].

Table 1. Penetrating-flux equations

<p>Combining</p> <ol style="list-style-type: none"> <li>1. Penetration equations [<math>m = f(P)</math>]</li> <li>2. Flux equations [<math>N = f(m)</math>]</li> </ol> <p>yields penetrating-flux equations</p> $N_{\text{penetrating}} = \phi = f(P)$ <p>where</p> <p><math>\phi</math> = flux of particles penetrating to a depth <math>P</math>, or greater, penetrations/unit area/unit time</p> <p><math>P</math> = penetration depth</p>
--

Given a combined flux-penetration equation  $\phi = f(P)$ , it is possible to calculate the probability of one or more meteoroid penetrations of a target as a function of  $P$ , target surface area exposed to the flux ( $A$ ), and time of exposure ( $T$ ). The probability of one or more penetrations to a depth  $P$ , or greater, is equal to  $\phi AT$ , provided that  $\phi AT$  is much less than one.<sup>5</sup>

<sup>5</sup>The equation for probability of zero penetrations to depth  $P$  is

$$\begin{aligned} \text{Prob}(0) &= (\phi AT)^0 e^{-\phi AT} / 0! \\ &= 1 - \phi AT \text{ when } \phi AT \ll 1 \end{aligned}$$

With the same restriction, the probability of one or more penetrations to depth  $P$  is equal to  $\phi AT$ .

The Whipple near-Earth flux equation has been combined with the penetration equations for copper and steel (Cf. Section II) to give combined flux-penetration equations for these two materials.

$$\phi = \left( \frac{P}{1.69} \right)^{-4.02} \times 10^{-12.45} \quad \text{for a copper target and a particle density of approximately } 2 \text{ g/cm}^3$$

$$\phi = \left( \frac{P}{1.41} \right)^{-4.02} \times 10^{-12.45} \quad \text{for a stainless steel target and a particle density of approximately } 2 \text{ g/cm}^3$$

$$\phi = \left( \frac{P}{0.837} \right)^{-4.02} \times 10^{-10.58} \quad \text{for a stainless steel target and a particle density of } 0.44 \text{ g/cm}^3$$

where

$\phi$  = flux of particles penetrating to a depth  $P$ , or greater, *penetrations/ft<sup>2</sup>-day*

$P$  = depth of penetration, in *centimeters*

The synthesis of a combined flux-penetration equation for meteoroid masses greater than  $10^{-6}$  g is more difficult for deep space than for near Earth. For the calculations of probability of solid-propellant motor puncture for an unmanned Mars mission (Section V), it is assumed that the ratio

$$\frac{\text{near-Earth flux}}{\text{deep-space flux}}$$

decreases from  $10^2$  at  $m = 10^{-6}$  g to 1 at  $m = 10^{-1}$  g. The resulting relation for  $m = 10^{-6}$  to 1 g is

$$\log \frac{\text{near-Earth flux}}{\text{deep-space flux}} = -0.4 - 0.4 \log m$$

The shortcomings in the synthesis of combined flux-penetration equations are the lists of missing data and correlations. These are summarized below:

*Meteoroid Data*

Refined values of flux as a function of mass, of position, of year, and of time of year.

*Penetration Data*

$P/d$  for actual structural materials as functions of projectile diameter, velocity, density, shape, incidence angle, and for thin and thick targets.

There is an additional list of data needed to determine pressure-vessel failure criteria.



#### IV. APPLICABILITY OF THE EXPLORER XVI DATA

The *Explorer XVI* Earth-satellite pressure-cell experiments are unique in that they are the only experiments to date in which the number of penetrations as a function of target thickness and time have been directly measured. It is of interest to examine the applicability of *Explorer XVI* data to the prediction of probability of critical meteoroid penetration of solid-propellant motors near Earth.

Figure 3 shows *Explorer XVI* spacecraft configuration. The primary experiment aboard this spacecraft was Langley Research Center's pressurized-cell micrometeoroid detector. A total of 160 annealed

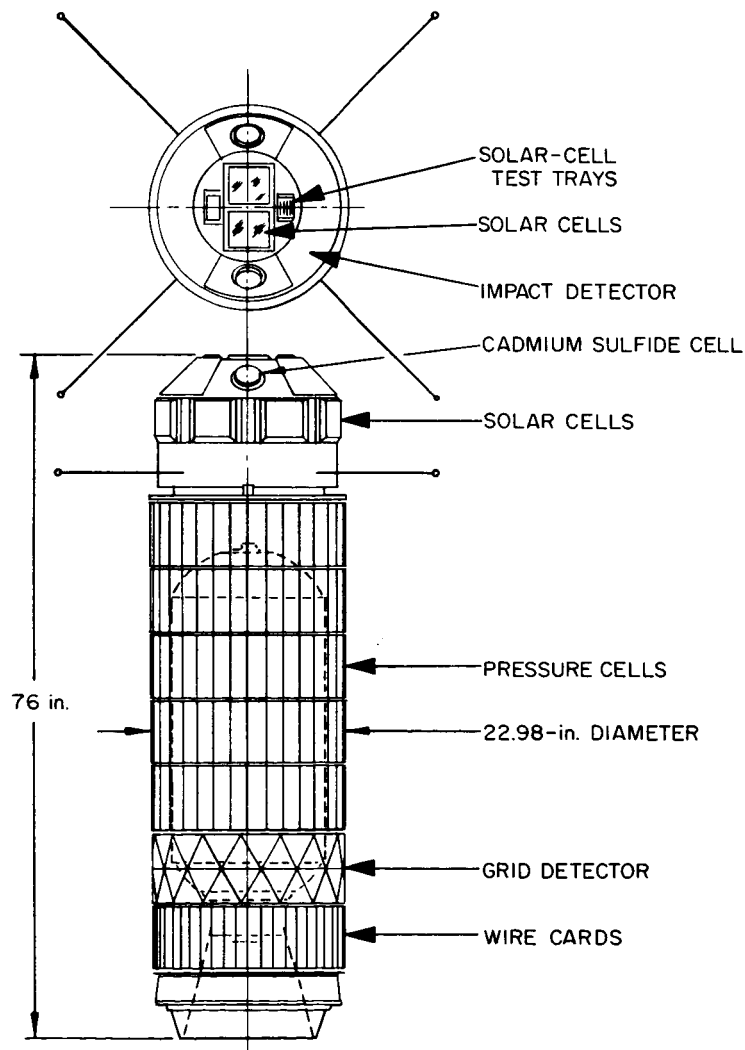


Fig. 3. *Explorer XVI*: spacecraft configuration

Be-Cu cells were mounted around the periphery of the spent rocket motor case in 5 rows of 32 cells each. These cells had external skin thicknesses of 0.001, 0.002, or 0.005 in., distributed as follows:

<u>Cell Dimensions</u>	<u>Number of Cells</u>
0.001-in. cells for a total surface area of 10.625 ft <sup>2</sup>	100
0.002-in. cells for a total surface area of 4.250 ft <sup>2</sup>	40
0.005-in. cells for a total surface area of 2.125 ft <sup>2</sup>	20

Each cell was filled with helium, and puncture was indicated by a pressure decrease.

Data from *Explorer XVI* were received for 219 days, during which the following punctures were recorded (Refs. 4, 5, 6, and 7).

44 punctures of 0.001-in. cells  
 11 punctures of 0.002-in. cells  
 NO punctures of 0.005-in. cells

To obtain a value for the penetrating flux from these data, it was necessary to normalize the actual number of punctures,  $p$ , to the value expected for some constant surface area. The accumulated punctures normalized to the initial surface area  $A_0$  are shown in Fig. 4. Note that the slope is decreasing with increasing number of days, which illustrates the periodic nature of meteoroid flux. The resulting average penetrating flux for these pressure cells is shown in Fig. 5. The maximum likelihood fit and the confidence limits are Langley's.

Langley has also reported some penetration data at velocities less than 5 km/sec for both the Be-Cu alloy used in the pressure cells and for Al. The data showed that the penetration depth in Al was approximately twice that for Be-Cu, indicating that, for these velocities, the Be-Cu behaves much like Cu<sup>6</sup>

Figure 6 compares the calculated fluxes of penetrating particles for copper and steel (Section III) with that measured by *Explorer XVI*. Note that the calculated values are for a thick target at normal incidence angles, which is only an approximation of a thin target at actual incidence angles. (The *Explorer* data are, of course, measured values for a thin target at actual incidence angles.) Although Whipple's most recent meteoroid-density estimate is 0.44 g/cm<sup>3</sup>, this density value is uncertain, and the corresponding uncertainty in the calculated penetrating flux is high. The effect of meteoroid density on penetrating flux for a steel target is illustrated in Fig. 6.

<sup>6</sup>Based on Scully's data for Cu and Al.

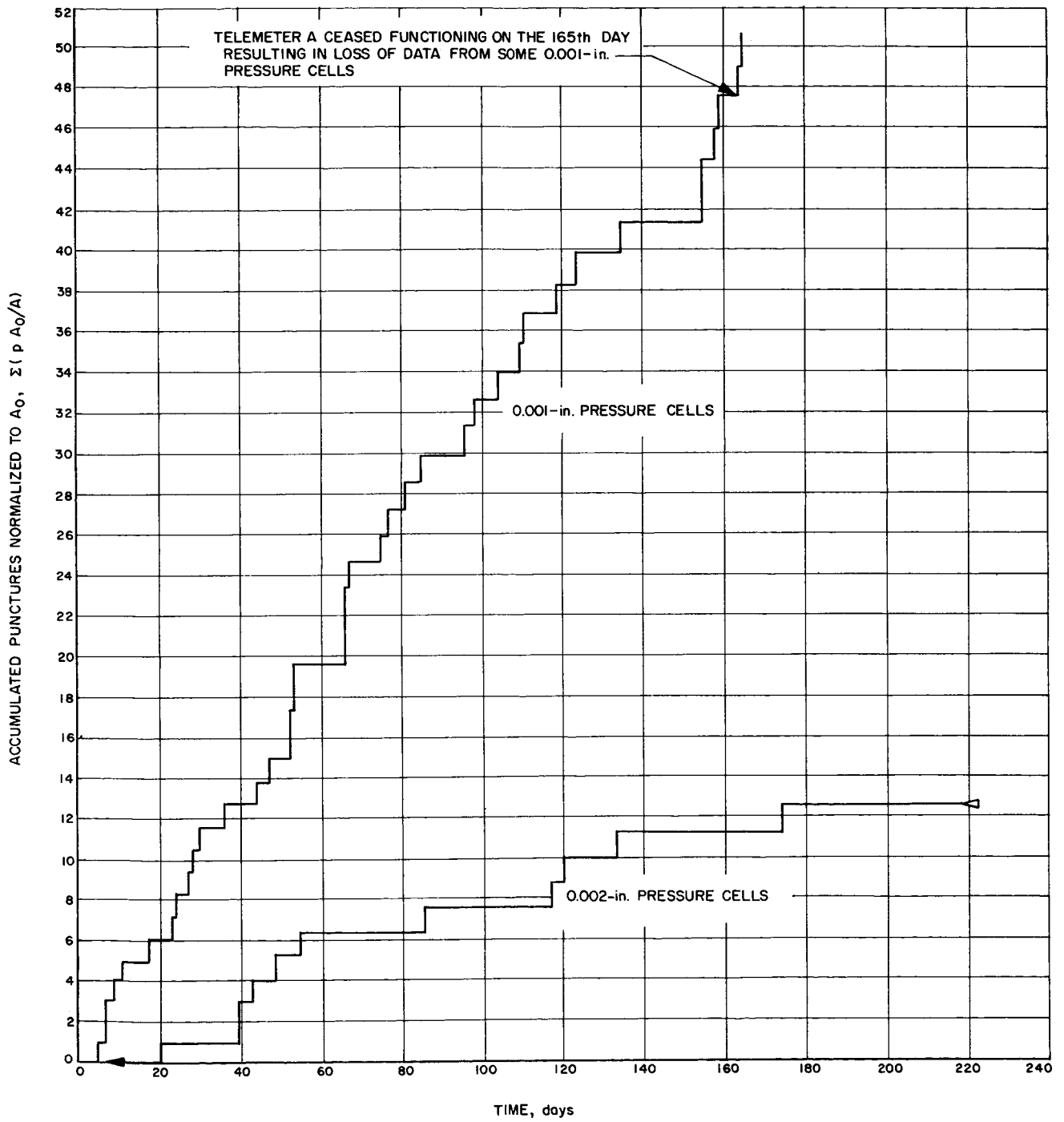


Fig. 4. Explorer XVI: normalized accumulated punctures vs time in orbit

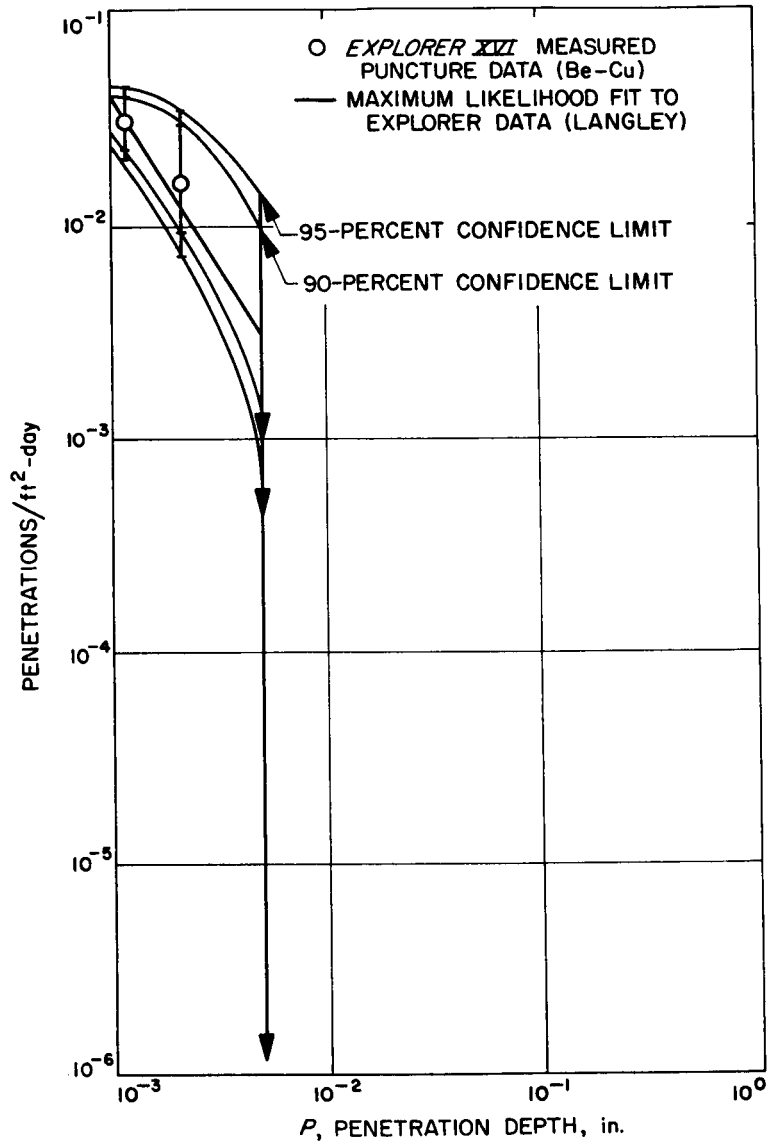


Fig. 5. Explorer XVI: near-Earth flux of penetrating particles vs penetration depth

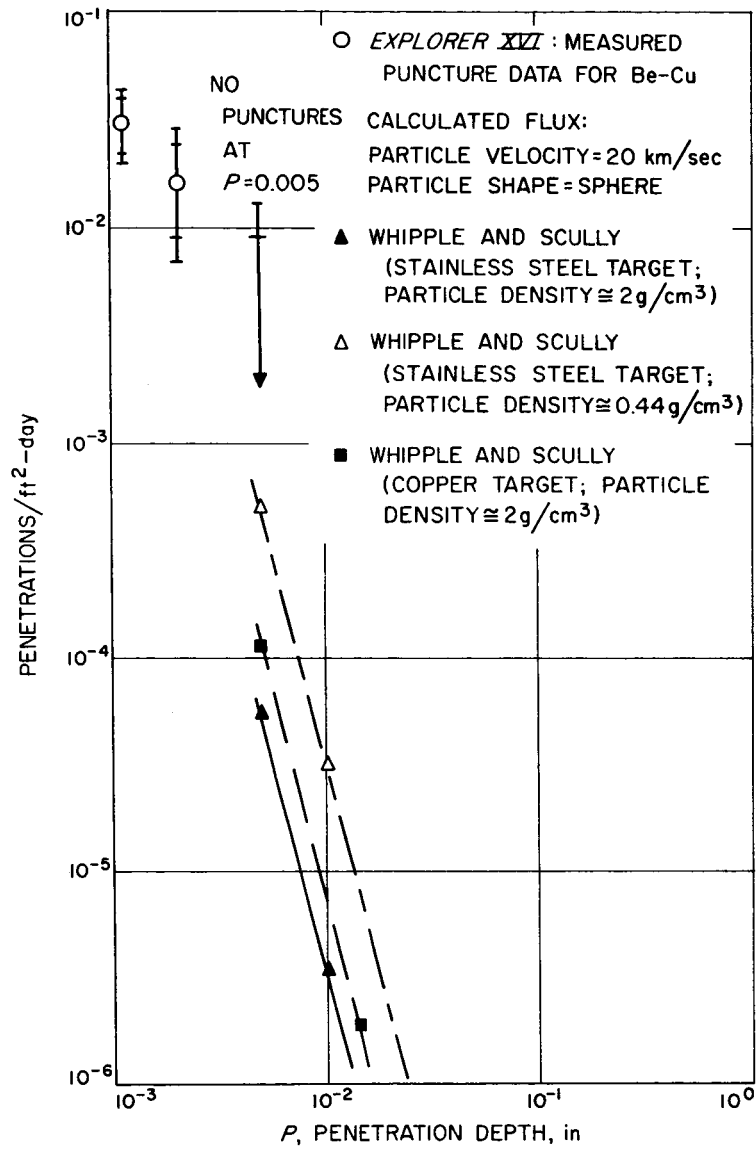


Fig. 6. Near-Earth flux of penetrating particles vs penetration depth: comparison of calculated values with Explorer XVI values

Because the 0.005-in. cell suffered no punctures, the *Explorer XVI* data are totally applicable only below a target thickness of 0.002-in. of Be-Cu, which is probably equivalent to less than 0.002-in. of steel. The calculated flux of penetrating particles, on the other hand, is valid only above meteoroid masses of approximately  $10^{-6}$  g, which, for a meteoroid density of  $0.44 \text{ g/cm}^3$  and velocity of 20 km/sec hitting a steel target, corresponds to a penetration depth of 0.005-in., or greater.

The minimum critical-penetration depth applicable to solid propellant motors depends not only on the case thickness, but also on the failure criteria. However, for the majority of applications the minimum depth is probably 0.005-in., or greater, as demonstrated in Section V.

As discussed in Section III, it is difficult to synthesize a credible equation for the flux of particles which would severely damage solid rocket motors. But, for the same reasons, we are unable to utilize the *Explorer XVI* data, which would require extrapolations to much greater material thicknesses and to materials other than Be-Cu.

## V. CONCLUSIONS

The degree of concern about meteoroid damage to solid-propellant motors depends on the probability of critical punctures of solid-propellant motors for typical missions. To provide some crude assessment of this hazard, we have estimated the probability of critical penetration for a small and a large solid-propellant spacecraft motor for a typical unmanned Mars mission. The results of these calculations are shown in Table

2. The assumptions and input data were as follows:

### *Meteoroid environment*

Near-Earth flux; Whipple, 1963

$$\text{Deep-space flux; } \log \left( \frac{\text{near-Earth flux}}{\text{deep-space flux}} \right) = -0.4 - 0.4 \log m$$

Meteoroid shape; sphere

Meteoroid density; 0.44 g/cm<sup>3</sup>

Meteoroid velocity; 20 km/sec

Incidence angle; 45 deg

### *Penetration criteria*

$P/d$  for a steel target; Scully's data for semi-infinite stainless steel target at normal incidence

Effect of particle density;  $P/d$  is proportional to the two-thirds power of the particle density<sup>7</sup>

Penetration depth for thin target at 45 deg incidence angle = penetration depth for semi-infinite target at normal incidence

### *Failure criteria*

Penetration to one-half the case thickness constitutes failure.

For penetration to one-half the case thickness, the  $P/d$  ratio is closer to the thin-sheet value than to the semi-infinite solid value.

---

<sup>7</sup>To convert Scully data from a projectile density of  $\sim 2$  g/cm<sup>3</sup> to a density of 0.44 g/cm<sup>3</sup>.

Table 2. Probability of sustaining one or more critical penetrations during an unmanned Mars mission

$$v = 20 \text{ km/sec}$$

$$\rho = 0.44 \text{ g/cm}^3$$

Critical penetration distance =  $P$  = one-half case or wall thickness

Case material	Propulsion system characteristics					Percent probability of one or more critical penetration			Minimum meteoroid mass required for critical penetration, g
	Propellant mass, lb	Chamber pressure, psia	Chamber-wall thickness, in.	Chamber surface area, ft <sup>2</sup>	Near Earth, <sup>a</sup> 1 day	Deep space, 230 days	Total mission		
Steel	24	250	0.010	2.2	0.12%	0.46%	0.58%	$3.5 \times 10^{-6}$	
Steel	760	250	0.030	19.6	0.013%	0.18%	0.19%	$9.5 \times 10^{-5}$	

<sup>a</sup>The full near-Earth flux is assumed to extend to approximately 20 Earth radii (24 hr for a typical unmanned Mars trajectory).



Some of the above assumptions appear optimistic, others pessimistic. For example, large uncertainties in the calculated probabilities arise from the uncertainties in the failure criteria. These criteria seem pessimistic for materials that are ductile and optimistic for materials that are brittle under high rates of loading.

The most interesting observations about probability of puncture of solid-propellant rocket motor cases, however, depend only on the slope of the penetrating-flux curve and not on the magnitude of the flux, as explained in Table 3 (Ref. 8). The probability of puncture is proportional to the slope ( $-n$ ) of the penetrating flux vs penetration-depth curve. Provided  $n$  is greater than two, the probability of puncture decreases with increasing motor-case radius and with increasing chamber pressure. The probabilities given in Table 2 show that if the flux for meteoroid masses greater than  $10^{-6}$  g is dependent on position in space, then the effective value of  $n$  (and the effect of motor-case diameter and pressure) will be mission or mission-phase dependent. For example, for an Earth-satellite mission, Table 2 shows that

$$\phi AT \sim \frac{\text{time}}{(\text{chamber radius})^2 (\text{chamber pressure})^4}$$

But, for a mission involving an Earth-Mars transit

$$\phi AT \sim \frac{\text{time}}{(\text{chamber radius})^1 (\text{chamber pressure})^3}$$

Note that it has been assumed in the above discussion that the failure criteria are independent of motor size and chamber pressure, and that the meteoroid characteristics, such as density and velocity, are independent of mass and of position in space.

In summary, the probabilities in Table 2 may be in error by more than an order of magnitude. They do, however, show a basis for concern, and they suggest that higher chamber pressures at a small loss in performance may be a good investment.

**Table 3. Pressure vessels**  
**Effect of size and pressure on probability of penetration**

$$\phi AT \sim P^{-n} AT \sim \frac{(\text{chamber radius})^2 (\text{time})}{(\text{chamber thickness})^n}$$

Chamber thickness  $\sim$  (chamber pressure) (chamber radius)

$$\phi AT \sim \frac{(\text{chamber radius})^2 (\text{time})}{(\text{chamber pressure})^n (\text{chamber radius})^n}$$

$$\phi AT \sim \frac{(\text{chamber radius})^{2-n} (\text{time})}{(\text{chamber pressure})^n}$$

## NOMENCLATURE

$A$	target surface area
$C$	constant
$d$	diameter of meteoroid or projectile
$m$	mass of meteoroid or projectile
$n$	absolute value of slope of penetrating flux vs penetration depth curve
$N$	flux of all particles of mass $m$ , or greater, number of particles/unit area/unit time
$p$	number of punctures
$P$	penetration depth in the target
$T$	time
$v$	velocity of meteoroid or projectile
$Z$	absolute value of slope of cumulative flux vs meteoroid mass curves
$\phi$	flux of particles penetrating to a depth $P$ , or greater, penetrations/unit area/unit time
$\rho$	density of meteoroid or projectile

## REFERENCES

1. Whipple, F. L., "On Meteoroids and Penetration," *Advances in the Astronautical Sciences*, Vol. 13, January 1963, pp. 590-598.
2. Jaffe, L. D., and Rittenhouse, J. B., "Behavior of Materials in Space Environments," *ARA Journal*, March 1962, pp. 320-346.
3. Dubin, M., *Meteoroid Effects on Space Exploration*, NASA TN-D-1839, October 1963.
4. Hastings, H. C., *The Explorer XVI Micrometeoroid Satellite - Description and Preliminary Results for the Period December 16, 1962 Through January 13, 1963*. NASA TM X-810, February 1963.
5. Hastings, H. C., *The Explorer XVI Micrometeoroid Satellite - Supplement I*, NASA TM X-824, April 1963.
6. Hastings, H. C., *The Explorer XVI Micrometeoroid Satellite - Supplement II*, NASA TM X-899, September 1963.
7. Hastings, H. C., *The Explorer XVI Micrometeoroid Satellite - Supplement III*, NASA TM X-949, March 1964.
8. Gardner, R. E. and Robillard, C. L., *Meteoroid Environment and Possible Damage to Pressure Vessels*, JPL Space Programs Summary No. 37-24, Vol. IV, December 31, 1963, pp. 85-88.